ISSN 1070-3632, Russian Journal of General Chemistry, 2021, Vol. 91, No. 1, pp. 98–107. © Pleiades Publishing, Ltd., 2021.
Russian Text © The Author(s), 2021, published in Zhurnal Obshchei Khimii, 2021, Vol. 91, No. 1, pp. 125–135.

Synthesis, Structure, and Biological Activity of Mixed-Ligand Amine-Containing Copper(II) Coordination Compounds with 2-(2-Hydroxybenzylidene)-*N*-(prop-2-en-1-yl)hydrazinecarbothioamide

A. P. Gulea[a], V. O. Graur[a], Ia. I. Ulchina[a,*], P. N. Bourosh[b], V. A. Smaglii[c], O. S. Garbuz[a,d], and V. I. Tsapkov[a]

[a] *State University of Moldova, Chisinau, MD-2009 Moldova*
[b] *Institute of Applied Physics, Chisinau, MD-2028 Moldova*
[c] *Institute of Chemistry, Chisinau, MD-2028 Moldova*
[d] *Institute of Zoology, Chisinau, MD-2028 Moldova*
**e-mail: ianina.ulchina@gmail.com*

Received October 2, 2020; revised October 2, 2020; accepted October 17, 2020

Abstract—Copper(II) nitrate reacts in ethanol with 2-(2-hydroxybenzylidene)-*N*-(prop-2-en-1-yl)hydrazinecarbothioamide H_2L in an 1 : 1 molar ratio to form the coordination compound $Cu(HL)NO_3 \cdot H_2O$. The introduction of amines [imidazole (Im), 3,5-dibromopyridine (3,5-Br_2Py), and 4-methylpyridine (4-Pic)] into the reaction mixture in a molar ratio 1 : 1 : 2 leads to the formation of $CuA(HL)NO_3 \cdot nH_2O$ [A = Im, 3,5-Br_2Py, 4-Pic; n = 0, 3] complexes. The structure of the obtained compounds was determined by X-ray structural analysis. The synthesized complexes exhibit antimicrobial, antifungal, antioxidant, and anticancer activities.

Keywords: Cu(II) coordination compounds, amines, salicylaldehyde 4-allylthiosemicarbazone, antimicrobial activity, anticancer activity

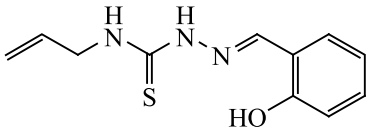
DOI: 10.1134/S1070363221010114

Thiosemicarbazones and coordination compounds of transition metals with them are biologically active compounds [1–3]. Many of them exhibit antimicrobial, antifungal, and anticancer activities [4–6]. In most cases, the coordination of thiosemicarbazones to copper(II) ions leads to the most significant increase in biological activity compared to ions of other 3*d* metals. A number of studies [7–9] have shown that the introduction of various amines into the inner sphere of copper(II) thiosemicarbazonates leads to a change in their biological properties. In this regard, it is of interest to synthesize and study new mixed-ligand amino-containing copper(II) coordination compounds with thiosemicarbazones.

We have synthesized copper(II) coordination compounds with 2-(2-hydroxybenzylidene)-*N*-(prop-2-en-1-yl)-hydrazinecarbothioamide (H_2L, Scheme 1) and such amines as imidazole (Im), 3,5-dibromopyridine (3,5-Br_2Py), and 4-methylpyridine (4-Pic), have determined their composition and structure, and studied their physicochemical and biological properties.

When a hot (50–55°C) ethanol solution of thiosemicarbazone H_2L reacts with an ethanol solution of copper(II) nitrate in a molar ratio of 1 : 1, a fine-crystalline compound of the composition $Cu(HL)NO_3 \cdot H_2O$ (**1**) is formed. For the synthesis of copper complexes containing heteroaromatic amines, the reactions of ethanol solutions of thioamide H_2L with copper(II) nitrate and amines

Scheme 1.



H_2L

(imidazole, 3,5-dibromopyridine, 4-methylpyridine) in a molar ratio of 1 : 1 : 2 were carried out. As a result, three amino-containing complexes **2**–**4** of the composition $CuA(HL)NO_3 \cdot nH_2O$ [A = Im (**2**), 3,5-Br_2Py (**3**), and 4-Pic (**4**), n = 0 (**2**, **3**), 3 (**4**)] were obtained.

Resulting coordination compounds **1**–**4** are insoluble in diethyl ether, slightly soluble in water, better in alcohols, and well soluble in DMFA and DMSO. Determination of the molar electrical conductivity (æ) of the synthesized complexes in methanol showed that compounds **1**–**4** are binary electrolytes of the 1 : 1 type (æ = 92–103 Ω^{-1} cm^2 mol^{-1}) (Table 1).

A magnetochemical study of the synthesized coordination compounds showed that complexes **1**–**4** have an underestimated value of the effective magnetic moment (μ_{ef} = 1.42–1.50 BM, Table 1) compared to the spin only value for a single unpaired electron, which points to their poly-nuclear structure.

To determine the mode of thiosemicarbazone coordination to copper(II) ions, a comparative analysis of the IR spectra of the H_2L ligand and complexes **1**–**4** was performed. The spectra of the synthesized compounds contain absorption bands in the regions of 3380–3100, 1630–1570, and 1400–1100 cm^{-1} which characterize the stretching vibrations of the coordinated molecules of the corresponding ligands. In the region of 3380–3100 cm^{-1} the ν(O–H) absorption band of the phenol group disappears from the IR spectra of all the complexes, which points to deprotonation of the H_2L ligand molecule as a result of coordination. In addition, the spectra show shifts of the ν(C=N) absorption band to the low–frequency region by 18–25 cm^{-1} and of the ν(C=S) absorption band to the high-frequency region by 24–38 cm^{-1}. It points to the coordination of the H_2L ligand to the central atoms by means of the deprotonated phenolic oxygen atom, the azomethine nitrogen atom, and the sulfur atom in the thionic form. In the IR spectra of all the complexes, a number of new absorption bands appear in the region of 510–415 cm^{-1} caused by the ν(Cu–N), ν(Cu–O), and ν(Cu–S) vibrations.

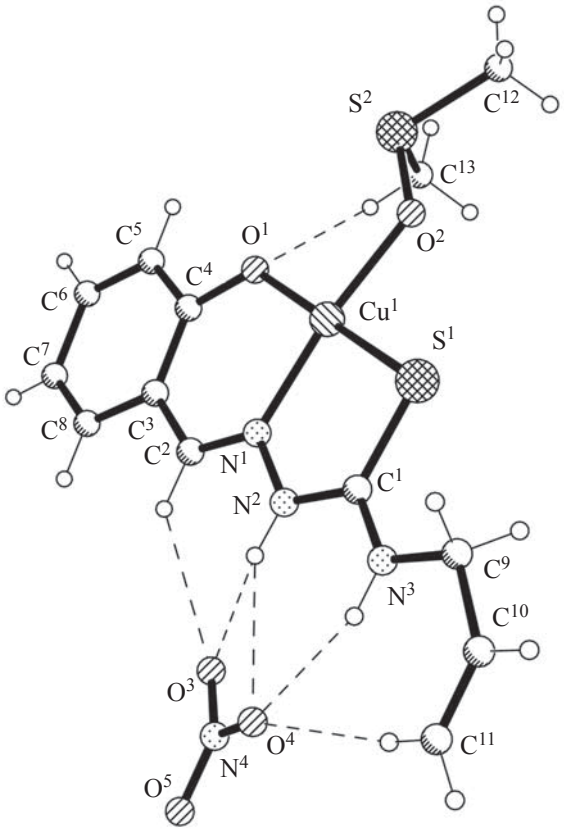


Fig. 1. General view of a complex **1a** in a crystal.

During recrystallization of complex **1** from DMSO and of complexes **2**–**4** from ethanol, single crystals were obtained, the structure of which was determined by X-ray structural analysis. Compound **1a** obtained by recrystallization of complex **1** from DMSO crystallizes in the $P\bar{1}$ triclinic space group (Table 2). The independent part of the crystal unit cell contain the complex cation $[Cu(DMSO)(HL)]^+$ and the NO_3^- anion. Thus, the recrystallization of polynuclear complex **1** from DMSO

Table 1. Physicochemical characteristics of copper coordination compounds with 2-(2-hydroxybenzylidene)-*N*-(prop-2-en-1-yl)-hydrazinecarbothioamide

Comp. no.	Yield, %	μ_{ef}[a], BM	æ,[a] Ω^{-1} cm^2 mol^{-1}	Found, %			Formula	Calculated, %		
				Cu	N	S		Cu	N	S
1	71	1.50	103	16.97	15.02	8.69	$C_{11}H_{14}CuN_4O_5S$	16.82	14.83	8.49
2	72	1.47	97	14.63	19.84	7.70	$C_{14}H_{16}CuN_6O_4S$	14.85	19.64	7.49
3	85	1.42	96	10.53	11.16	5.48	$C_{16}H_{15}Br_2CuN_5O_4S$	10.65	11.74	5.37
4	83	1.50	92	12.36	14.15	6.60	$C_{17}H_{25}CuN_5O_7S$	12.53	13.81	6.32

[a] At 293 K.

Table 2. Crystallographic characteristics, experimental data, and refinement of the structures of complexes **1a** and **2–4**

Parameter	**1a**	**2**	**3**	**4**
Chemical formula	$C_{13}H_{18}Cu_1N_4O_5S_2$	$C_{28}H_{32}Cu_2N_{12}O_8S_2$	$C_{32}H_{30}Br_4Cu_2N_{10}O_8S_2$	$C_{34}H_{50}Cu_2N_{10}O_{14}S_2$
M	437.97	855.85	1193.50	1014.04
Crystal System	Triclinic	Triclinic	Triclinic	Orthorhombic
Space group	$P\bar{1}$	$P\bar{1}$	$P\bar{1}$	*Pnna*
Z	2	1	1	4
a, Å	4.4503(5)	7.4237(6)	7.1201(7)	26.5825(13)
b, Å	12.5530(12)	11.4130(9)	12.7325(11)	22.4006(10)
c, Å	17.0921(18)	11.8704(11)	13.0483(10)	7.5445(7)
α, deg	108.339(9)	113.657(9)	114.097(8)	90
β, deg	93.073(9)	98.037(8)	96.429(8)	90
γ, deg	91.077(9)	97.209(7)	100.090(8)	90
V, Å^3	904.40(18)	893.70(14)	1040.73(17)	4492.5(5)
D_{calc}, g/cm^3	1.608	1.590	1.904	1.499
μ, cm^{-1}	1.470	1.372	5.022	1.113
F(000)	450	438	586	2104
Sample size, mm	0.08×0.04×0.03	0.45×0.14×0.06	0.4×0.09×0.04	0.6×0.05×0.015
θ_{max}, deg	3.25–25.05	3.07–25.05	2.97–25.50	2.95–25.04
Limits of *h*, *k*, *l*	$-5 \le h \le 5$, $-14 \le k \le 14$, $-20 \le l \le 15$	$-8 \le h \le 8$, $-13 \le k \le 9$, $-13 \le l \le 14$	$-8 \le h \le 8$, $-12 \le k \le 15$, $-15 \le l \le 15$	$-31 \le h \le 29$, $-16 \le k \le 26$, $-8 \le l \le 8$
Measured/indendent reflexes	4883	4348	5800	14413
	3194 [*R*(int) 0.0762]	3082 [*R*(int) 0.0213]	3847 [*R*(int) 0.0203]	3954 [*R*(int) 0.0736]
Reflexes with $I > 2\sigma(I)$	1175	2309	2979	2251
GOOF	1.001	1.002	1.001	1.008
R-factors with $I > 2\sigma(I)$	R_1 0.0847,wR_2 0.1358	R_1 0.0466,wR_2 0.0873	R_1 0.0374,wR_2 0.0899	R_1 0.0733,wR_2 0.1583
R-factors for the whole array	R_1 0.2269, wR_2 0.1894	R_1 0.0718, wR_2 0.0979	R_1 0.0551, wR_2 0.0972	R_1 0.1372, wR_2 0.1853
$\Delta\rho_{max}/\Delta\rho_{min}$, *e*/Å^3	0.426/–0.400	0.276/–0.262	0.538/–0.408	0.466/–0.273

resulted in the formation of the mononuclear compound $[Cu(DMSO)(HL)]NO_3$ **1a** containing a coordinated DMSO molecule (Fig. 1). Thiosemicarbazone acts as a tridentate monodeprotonated ligand and is coordinated to the central metal atom using the ONS set of donor atoms to form two metal cycles: a five-membered thiosemicarbazide and a six-membered salicylidene. The fourth coordination place of the Cu^1 atom is occupied by the O atom of the DMSO molecule, and its coordination polyhedron formed by the O_2NS set of donor atoms is a distorted square. In this case, the deviation of the coordinated atoms from the mean plane is ±0.05 Å.

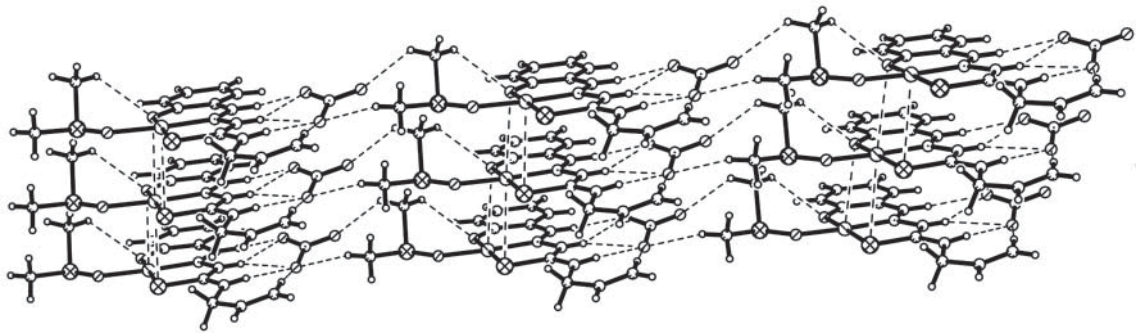


Fig. 2. Formation of stacks of complex cations and formation of a layer in complex **1a.**

Table 3. Interatomic distances and valence angles in Cu(II) coordination polyhedra of compounds **1a** and **2**–**4**[a]

Bond	*d*, Å			
	1a	**2**	**3**	**4**
$Cu^1–N^1$	1.933(8)	1.954(3)	1.971(3)	1.957(5)
$Cu^1–O^1$	1.896(7)	1.925(2)	1.926(3)	1.923(4)
$Cu^1–S^1$	2.263(3)	2.294(1)	2.295(1)	2.279(2)
$Cu^1–O^2/N^4$	1.952(6)	1.961(3)	2.044(3)	2.000(6)
$Cu^1–O^{1*}$		2.703(1)	2.405(1)	2.664(1)
Angle		ω, deg		
$N^1Cu^1O^1$	93.1(3)	90.8(1)	89.26(12)	92.57(2)
$N^1Cu^1S^1$	87.0(3)	85.31(9)	84.76(10)	85.4(2)
$N^1Cu^1O^2/N^4$	173.3(4)	174.9(1)	171.07(12)	172.5(2)
$N^1Cu^1O^{1*}$	–	94.3(4)	99.96(11)	90.7(1)
$O^1Cu^1S^1$	178.3(3)	176.08(8)	173.74(8)	177.9(1)
$O^1Cu^1O^2/N^4$	92.1(3)	90.0(1)	90.00(12)	89.1(2)
$O^1Cu^1O^{1*}$	–	83.7(9)	81.00(10)	82.9(1)
$S^1Cu^1O^2/N^4$	87.9(2)	93.89(9)	96.19(9)	93.0(1)
$S^1Cu^1O^{1*}$	–	95.8(10)	98.17(7)	96.9(3)
$N^4Cu^1O^{1*}$	–	90.9(9)	88.71(10)	96.8(3)

[a] * $-x+1, -y+1, -z$ (**2**); $-x+1, -y+1, -z+1$ (**3**); $x, -y+3/2, -z+1/2$ (**4**).

The $Cu–O^1$, $Cu–N^1$, and $Cu–S^1$ interatomic distances of 1.896(7), 1.933(8), and 2.263(3) Å correspond to the values for similar compounds [3, 10, 11]; the $Cu–O^2$ distance is 1.952 (6) Å (Table 3).

In the crystal of compound **1a**, complex cations are associated in a stack along the *a* axis by means of weak interactions $Cu^1\cdots O^1$ ($x+1, y, z$) 3.525 Å and $Cu^1\cdots S^1$ ($x–1, y, z$) 3.505 Å, the $Cu^1\cdots Cu^1$ ($x+1, y, z$) interatomic distance being 3.525 Å (Figs. 2, 3). Complex cations are additionally stabilized by intramolecular hydrogen bonds $C^{13}–H\cdots O^1$ (Table 4). The anions NO_3^- are bound to a single cation both by protons of the HL^- ligand, forming intermolecular hydrogen bonds $N^2–H\cdots O^3$, $N^2–H\cdots O^4$, $N^3–H\cdots O^4$ and weak $C^2–H\cdots O^3$ and $C^{11}–H\cdots O^4$ bonds, and by C–H···O bonds of protons from methyl groups of DMSO molecules (Figs. 1–3, Table 4). In addition, separate layers can be distinguished in the crystal (Fig. 2), which are interconnected by C–H···S weak hydrogen bonds (Fig. 3).

The X-ray structural analysis showed that compounds **2**–**4**, as well as complex **1a**, are ionic, but they contain binuclear complex cations with charges compensated by the same NO_3^- anions. The crystals of compounds **2** and **3** contain no crystallization molecules of the solvent, whereas in complex **4** disordered water molecules occupying 10 positions were identified in the cations : anions ratio of 1 : 2 : 6 : water molecules.

Coordination compounds **2**–**4** crystallize in the $P\bar{1}$ space groups of triclinic and *Pnna* orthorhombic crystal systems (Table 2). The coordination formulas of these compounds are $[Cu_2(Im)_2(HL)_2](NO_3)_2$ (**2**), $[Cu_2(3,5\text{-}Br_2Py)_2(HL)_2](NO_3)_2$ (**3**), and $[Cu_2(4\text{-}Pic)_2(HL)_2](NO_3)_2 \cdot 6H_2O$ (**4**), i.e. all crystals contain binuclear complex cations $[Cu_2(A)_2(HL)_2]^{2+}$ (Fig. 4). The coordination polyhedra of copper atoms in complexes **2**–**4** are distorted square bipyramids with coordination numbers which can be described as 4+1+1. In the equatorial plane of the polyhedra there are the ONS set of atoms of the monodeprotonated HL^- ligand and the nitrogen atom of a corresponding amine: Im, 3,5-Br_2Py, or 4-Pic. In addition, the HL^- ligands function as bridges. A similar coordination mode of the HL^- ligand was found in the copper(II) trinuclear sulfate complex [12] and the

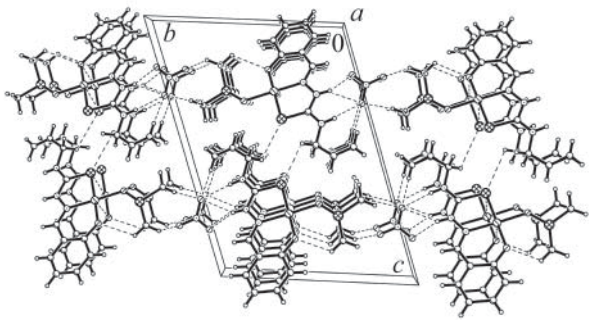


Fig. 3. Packing of layers in a compound **1a** crystal.

Table 4. Geometric parameters of hydrogen bonds for compounds **1a** and **2–4**

Contact D–H···A	Distance, Å			Angle DHA	Symmetry transformation for A atoms
	D–H	H···A	D···A		
1a					
N^2–H^2···O^3	0.86	1.92	2.74(1)	158	*x*, *y*, *z*
N^2–H^2···O^4	0.86	2.53	3.25(1)	141	*x*, *y*, *z*
N^3–H^3···O^4	0.86	2.06	2.89(1)	163	*x*, *y*, *z*
C^2–H^2···O^3	0.93	2.58	3.32(2)	137	*x*, *y*, *z*
C^{11}–H^{11A}···O^4	0.93	2.33	3.34(1)	165	*x*, *y*, *z*
C^{12}–H^{12B}···O^5	0.96	2.61	3.33(1)	133	*x*–1, *y*+1, *z*
C^{13}–H^{13C}···O^1	0.96	2.53	3.12(1)	120	*x*, *y*, *z*
C^{13}–H^{13B}···O^5	0.96	2.48	3.23(1)	134	*x*–1, *y*+1, *z*
2					
N^2–H^2···O^2	0.86	1.92	2.767(4)	167	*x*, *y*, *z*
N^3–H^3···O^4	0.86	2.05	2.899(4)	170	*x*, *y*, *z*
N^5–H^5···O^4	0.86	1.98	2.831(4)	169	*x*, *y*–1, *z*–1
C^2–H^2···O^2	0.93	2.56	3.319(5)	139	*x*, *y*, *z*
C^{10}–H^{10}···O^3	0.93	2.46	3.361(6)	164	–*x*, –*y*+2, –*z*+2
C^{12}–H^{12}···O^1	0.93	2.37	2.830(5)	110	*x*, *y*, *z*
3					
N^2–H^2···O^3	0.86	2.54	3.244(5)	139	*x*, *y*, *z*
N^2–H^2···O^4	0.86	1.91	2.733(4)	160	*x*, *y*, *z*
N^3–H^3···O^3	0.86	1.97	2.817(5)	169	*x*, *y*, *z*
C^2–H^2···O^4	0.93	2.48	3.243(5)	139	*x*, *y*, *z*
C^{12}–H^{12}···S^1	0.93	2.73	3.307(4)	121	*x*, *y*, *z*
C^{16}–H^{16}···O^1	0.93	2.24	2.802(5)	119	*x*, *y*, *z*
4					
N^2–H^2···O^2	0.86	2.54	3.243(5)	178	*x*, *y*, *z*
N^3–H^3···O^3	0.86	1.91	2.734(4)	180	*x*, *y*, *z*
C^{15}–H^{15}···O^4	0.93	2.45	3.371(8)	170	*x*–1/2, *y*, –*z*+1
C^9–H^{9B}···O^{7W}	0.97	2.75	3.607(4)	143	*x*, *y*, *z*
C^{16}–H^{16}···O^{5W}	0.93	2.73	3.419(5)	131	*x*, *y*, *z*

copper(II) binuclear nitrate complex with the N-methyl-substituted ligand [10]. As a result, the oxygen atom O^1 of the second HL^- ligand from this dimer is located in one of the axial positions of the metal polyhedra (Table 3). The second axial position of the coordination polyhedron is occupied by the sulfur atom S^1 of the neighboring dimer (Fig. 5). The interatomic distances of Cu–O^1, Cu–N^1, and Cu–S^1 in the coordination polyhedra of complexes

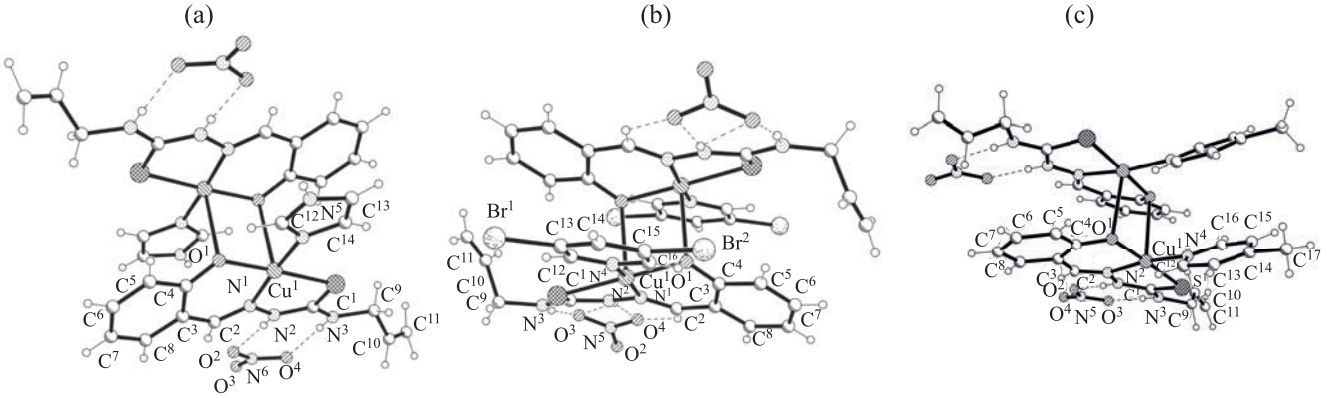


Fig. 4. General view of the molecules of binuclear complexes **2** (a), **3** (b), and **4** (c).

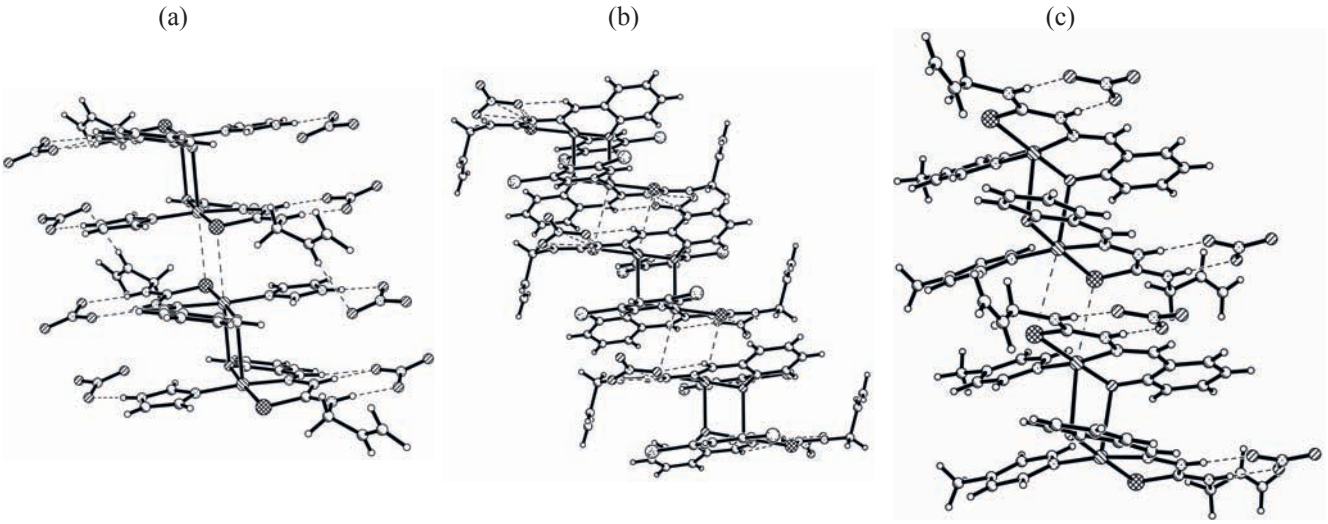


Fig. 5. Crystal packing of binuclear complex compounds **2** (a), **3** (b), and **4** (c).

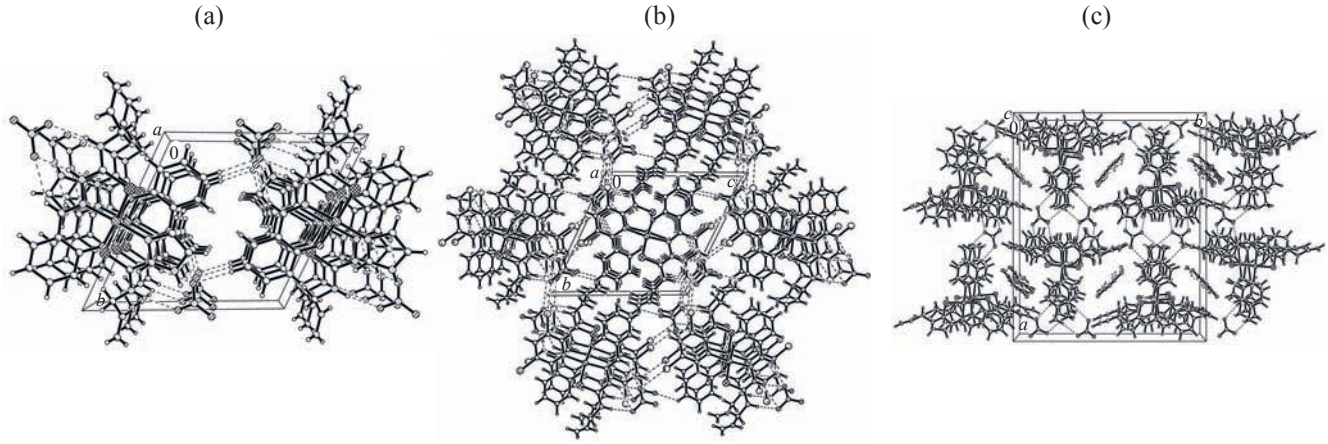


Fig. 6. Fragments of the crystal packing of compounds **2** (a), **3** (b) and **4** (c).

2–**4** are on average 1.925(3), 1.9614, and 2.289 (1) Å (Table 3), being similar to those found earlier [12] and slightly different from those found in complex **1a**, whereas the Cu–N^4, Cu–O^1*, Cu–S^1* distances lie in the intervals 1.961(3)–2.044(3), 2.405(1)–2.703(1), and 3.328(1)–3.484(1) Å, respectively. The geometric parameters of amines correspond to those found in copper complexes with similar ligands from the Cambridge Structural Data Base [13].

Stacks formed by binuclear complex cations with anions strung on them can be distinguished in all crystal structures of **2**–**4**. The interatomic distances $Cu^1 \cdots Cu^1$* are 3.486 and 3.957 Å (**2**), 3.308 and 3.853 Å (**3**), 3.462 and 4.102 Å (**4**) (Figs. 2, 3, 5). The cations themselves in the crystal are combined with the NO_3^- anions by the N^2–H···O, N^3–H···O and C–H···O^1 hydrogen bonds. Various groups of the HL^- ligands act as proton donors, and oxygen atoms of nitrate ions – as acceptors (Table 4, Figs. 4, 5). Complexes **2** and **3** are associated in a three-dimensional framework by means of the C–H···O hydrogen bonds with CH groups of both the HL^- ligands and amines acting as donors. In addition, layers formed by stronger N^5–H···O^4* hydrogen bonds can be distinguished in complex **2** (Fig. 6a). In complex **3**, Br···O interactions with interatomic distances of 3.017 and 3.169 Å can be additionally distinguished (Fig. 6b). The layers formed by means of C–H···O hydrogen bonds packed with the formation of cavities containing disordered water molecules can be noted in the structure of complex **4** (Fig. 6c). The calculation of the volume of cavities in **4** showed that they occupy 765.1 of 4492.5 $Å^3$ of the unit cell, which is greater by 17.0% compared to complex **2** (18.3 of 893.7 $Å^3$ of the unit cell, which is 2.0%). No

Table 5. Minimal suppressive concentration (MSC) and bactericidal/fungicidal (MBC/MFC) concentrations of coordination compounds **1**–**4** in relation to test microbes and fungi

Compound	*Eschirichia coli* ATCC 25922		*Klebsiella pneumoniae* ATCC 13883		*Staphylococcus aureus* ATCC 25923		*Candida albicans* ATCC 10231	
	MSC	MBC	MSC	MBC	MSC	MBC	MSC	MFC
	μg/mL							
$Cu(NO_3)_2 \cdot 3H_2O$	>1000	>1000	>1000	>1000	>1000	>1000	>1000	>1000
H_2L	>	>	>1000	>1000	7	60	>	>
1	>	>	>1000	>1000	>	>	>	>
2	30	60	500	500	30	30	30	30
3	120	120	250	500	250	250	30	30
4	3	3	120	250	30	60	30	30

Table 6. Antiproliferative activity of compounds H_2L and **1**–**3** against the HL-60 cell line of human myeloid leukemia

Compound	Inhibition of cell growth, %[a]			IC_{50}, μM
	10 μM	1 μM	0.1 μM	
H_2L	7.0	0	0	>10
1	100	0	0	5.0
2	97.6	96.6	7.6	0.32
3	96.8	94.9	25.4	0.28
Doxorubicin	99	98	15	0.50

[a] Average results of three experiments, SEM < ±4%.

Table 7. Antiproliferative activity of compounds H_2L and **1**–**3** against the HeLa cell line of cervical cancer

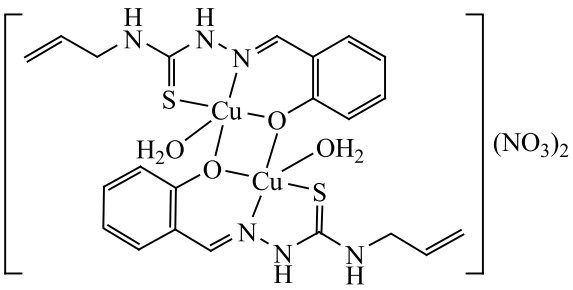
Compound	Inhibition of cell growth, %[a]			IC_{50}, μM
	10 μM	1 μM	0.1 μM	
H_2L	8.0	4.4	3.6	>10
1	100	13.6	11.9	1.3
2	88.3	0	0	7.0
3	100	0	0	5.0
Doxorubicin	49.8	12.2	0	10.0

[a] Average results of three experiments, SEM < ±4%.

cavities available for crystallization molecules were found in the crystals of compounds **1a** and **3**.

Based on the obtained physicochemical data, the distribution of chemical bonds in complex **1**, for which no single crystals were obtained, can be represented as follows (Scheme 2).

Scheme 2.



Antimicrobial and antifungal activities of thiosemicarbazone H_2L and coordination compounds **1**–**4** were studied *in vitro* against standard strains of the gram-positive microorganism *Staphylococcus aureus* (ATCC 25923), gram-negative microorganisms *Escherichia coli* (ATCC 25922) and *Klebsiella pneumonae* (ATCC 13883), and also of *Candida albicans* (ATCC 10231) as a representative of the fungi. It was found that the H_2L ligand does not show antimicrobial activity against gram-negative microorganisms and *Candida albicans*, but shows both bacteriostatic and bactericidal activities against *Staphylococcus aureus* in the concentration range of 7-60 μg/mL (Table 5). Complex **1** did not show activity against the studied strains of microorganisms. The synthesized amino-containing coordination compounds **2**–**4** exhibit antimicrobial and antifungal activity with the

Table 8. Concentrations IC_{50} of semi-maximal inhibition of the studied substances against MDCK, HL-60 and HeLa cells and *SI* selectivity indices

Compound	MDCK	HL-60		HeLa	
	IC_{50}, μM	IC_{50}, μM	*SI*[a]	IC_{50}, μM	*SI*[a]
H_2L	>10	>10	–	>10	–
1	6.0	5.0	1.2	1.3	4.6
2	12	0.32	37.5	7.0	1.7
3	9.0	0.28	32.1	5.0	1.8
Doxorubicin	7.1	0.50	14.2	10.0	0.71

[a] Index of selectivity of anti-cancer activity $SI = \frac{IC_{50}(\text{MDCK})}{IC_{50}(\text{cancer cells})}$.

values of minimal suppressive concentration (MSC) and minimal bactericidal concentration (MBC) in the range of 3–500 μg/mL. Consequently, coordination of amines led to a significant increase in antimicrobial activity against gram-negative microorganisms and antifungal activity. The most significant increase in activity against gram-negative microorganisms is observed in the case of complex **4** containing 4-methylpyridine.

Study of the antiproliferative activity of the H_2L ligand and compounds **1**–**3** against the HL-60 cancer cell lines of human myeloid leukemia (Table 6) and HeLa of cervical cancer (Table 7) showed that the H_2L compound shows almost no activity, suppressing the growth and reproduction of cancer cells by 7–8% at a concentration of 10 μM. Compound **1** inhibits the growth and reproduction of HL-60 cells by 100% at a concentration of 10 μM, and at lower concentrations (1 and 0.1 μM) it completely loses its activity. The introduction of amines into the inner sphere of copper(II) complexes **2** and **3** leads to increased activity against HL-60 cells. These complexes inhibit the proliferation of this type of cancer cells by almost 100% at concentrations of 10 and 1 μM, and also show a low activity at concentrations of 0.1 μM. In the case of HeLa cells, no increase in activity is observed.

Table 8 shows concentrations IC_{50} of half-maximal inhibition, which represent a measure of efficiency of antiproliferative action of the investigated substances in relation to HL-60 and HeLa cells and to model line of normal mammalian cells MDCK, and also indices of selectivity of anti-cancer activity, indicating how many times the activity against cancer cells is higher than in normal MDCK cells. The activity of complex **1** without amine in the inner sphere is significantly inferior in activity and selectivity to doxorubicin, which is used in medical practice as an anti-cancer substance. Amino-containing complexes **2**–**3** are 1.5–1.8 times more active than doxorubicin against HL–60 cells and 1.4–2 times more active than doxorubicin against HeLa cells. In addition, complexes **2** and **3** are superior to doxorubicin in selectivity for these cancer cell lines. Their effect on normal MDCK cells is 32.1–37.5 times weaker than that on HL-60 cancer cells.

The results of studying the antioxidant activity of compounds H_2L and **1**–**4** against $ABTS^{\bullet+}$ cation radicals are presented in Table 9 in the form of semi-maximal inhibition concentrations IC_{50}. The uncoordinated thiosemicarbazone H_2L shows higher activity than trolox, which is used in medical practice as a free radical inhibitor. Coordination of H_2L to the copper(II) ion (complex **1**) leads to a decrease in antioxidant activity, whereas the introduction of amines into the inner sphere (complexes **2**–**4**) re-increases antioxidant activity, and the activity of complexes with amines exceeds not only that of complex **1**, but also the activity of the initial thiosemicarbazone H_2L.

The above experimental data indicate the prospects for further search for selective antimicrobial, antifungal, and anticancer substances among copper mixed-ligand amino-containing coordination compounds with derivatives of thiosemicarbazone salicylic aldehyde.

Table 9. Antioxidant activity of compounds H_2L and **1**–**4** against cation radicals $ABTS^{\bullet+}$

Compound	IC_{50}, μM
H_2L	9.0
1	40
2	5.8
3	7.5
4	5.8
Trolox	33

EXPERIMENTAL

The X-ray diffraction data for complexes **1a** and **2**–**4** were obtained at 293(2) K on an Xcalibur E diffractometer with MoK_α radiation and a graphite monochromator. The unit cell parameters refined over the entire array and the rest of the experimental data were obtained using the CrysAlis Oxford Diffraction software package [14]. Their structures were solved by direct methods and refined by LSM in the anisotropic approximation for non-hydrogen atoms according to the SHELX-97 program [15]. Hydrogen atoms are included in the refinement in geometrically calculated positions, and their temperature factors U_H are assumed to be 1.2 or 1.5 times greater than those of the carbon, nitrogen, and oxygen atoms bound to them. The crystallization water molecules in complex **4** are localized in 10 positions with filling factors from 0.15 to 0.55. The main parameters of the experiment, the solution and refinement of structures are given in Table 2, interatomic distances and valence angles in coordination polyhedra—in Table 3, and the parameters of hydrogen bonds—in Table 4. The coordinates of the basic atoms of the studied structures are deposited in the Cambridge Data Bank (CCDC 2033700-2033703).

The resistance of solutions of complexes **1**–**4** in methanol (20°C, *c* 0.001 M) was measured using an R-38 rheochord bridge. The IR spectra of substances were recorded on a Bruker ALPHA spectrometer (4000–400 cm^{-1}). The effective magnetic moments of compounds **1**–**4** were determined by the Gouy method. The calculation of the molar magnetic susceptibility adjusted for diamagnetism was carried out on the basis of theoretical values of the magnetic susceptibility of organic compounds.

Antimicrobial, antifungal, antiproliferative, and antioxidant activities were studied according to standard methods described in [16, 17].

2-(2-Hydroxybenzylidene)-*N*-(prop-2-en1-yl)hydrazinecarbothioamide (H_2L) was obtained by the condensation reaction of *N*-(prop-2-en-1-yl)hydrazinecarbothioamide (4-allylthiosemicarbazide) with 2-hydroxybenzaldehyde (salicylic aldehyde) in accordance with the procedure described in [18].

Bis[μ$_2$-2-({2-[(prop-2-en-1-yl)carbamothioyl]hydrazinylidene}methyl)phenolato-*S*,*N*,*O*:*O*]-diaquadicopper(II) nitrate (1). To an ethanol solution containing 10 mmol of 2-(2-hydroxybenzylidene)-*N*-(prop-2-en-1-yl)hydrazine carbothioamide H_2L in 20 mL of alcohol, a solution containing 10 mmol of copper(II) nitrate trihydrate in 20 mL of ethanol was added with continuous stirring and heating (50–55°C). The resulting reaction mixture was stirred for 40–50 min. After cooling to room temperature, the formation of a fine crystalline substance was observed, which was filtered out on a glass filter, washed with a small amount of ethanol, and dried in air to a constant weight.

Bis[μ$_2$-2-({2-[(prop-2-en-1-yl)carbamothioyl]hydrazinylidene}methyl)phenolato-*S*,*N*,*O*:*O*]-diimidazoldicopper(II) nitrate (2). To a hot (50–55°C) ethanol solution (20 mL) containing 10 mmol of 2-(2-hydroxybenzylidene)-*N*-(prop-2-en-1-yl)hydrazinecarbothioamide H_2L, 10 mmol of copper(II) nitrate trihydrate was added. The resulting mixture was stirred with heating for 40–50 min, then an ethanol solution of 20 mmol imidazole was added to the resulting solution, and stirred with heating for another 30 min. When cooled, a precipitate was formed, which was filtered out, washed with a small amount of ethanol, and dried in air.

Compound 3 was synthesized similarly, using 3,5-dibromopyridine instead of imidazole.

Bis[μ$_2$-2-({2-[(prop-2-en-1-yl)carbamothioyl]-hydrazinylidene}methyl)phenolato-*S*,*N*,*O*:*O*]bis-(4-methylpyridine)dicopper(II) nitrate hexahydrate (4). To a hot (50–55°C) ethanol solution (20 mL) containing 20 mmol of 4-methylpyridine, 10 mmol of copper(II) nitrate trihydrate was added. The resulting mixture was stirred with heating for 30 min, then an ethanol solution of 10 mmol of 2-(2-hydroxybenzylidene)-*N*-(prop-2-en-1-yl)hydrazinecarbothioamide H_2L was added to the resulting solution and stirring with moderate heating was continued for 1 h. When cooled, a precipitate was formed, which was filtered out, washed with a small amount of ethanol, and dried in air.

ACKNOWLEDGMENTS

The authors express their gratitude to G.G. Balan and O.S. Burduniuc (N. Testemitsanu State Medical and Pharmaceutical University) for their assistance in conducting biological tests of synthesized substances.

FUNDING

The work was carried out within the framework of the state programs of the Republic Moldova (projects 20.80009.5007.10 and 20.80009.5007.15).

CONFLICT OF INTEREST

No conflict of interest was declared by the authors.

REFERENCES

1. Beraldo, H. and Gambino, D., *Mini Rev. Med. Chem*., 2004, vol. 4, no. 1, p. 31. https://doi.org/10.2174/1389557043487484
2. Joseph, J., Mary, N.L., and Sidambaram, R., *Synth. React. Inorg. Metal-Org. Nano-Metal Chem*., 2010, vol. 40, no. 10, p. 930. https://doi.org/10.1080/15533174.2010.522661
3. Gulea, A.P., Graur, V.O., Chumakov, Yu.M., Petrenko, P.A., Balan, G.G., Burduniuc, O.S., Tsapkov, V.I., and Rudic, V.F., *Russ. J. Gen. Chem*., 2019, 89, no. 5, p. 953. https://doi.org/10.1134/S1070363219050153
4. Lovejoy, D.B., *Blood*, 2002, vol. 100, no. 2, p. 666. https://doi.org/10.1182/blood.v100.2.666
5. Pelosi, G., *Open Crystallogr. J*., 2010, vol. 3, p. 16. https://doi.org/10.2174/1874846501003010016
6. Liberta, A.E. and West, D.X., *Biometals*, 1992, vol. 5, no. 2, p. 121. https://doi.org/10.1007/bf01062223
7. Prisakar', V.I., Tsapkov, V.I., Buracheeva, S.A., Byrke, M.S., and Gulea, A.P., *Pharm. Chem. J*., 2005, vol. 39, no. 6, p. 313. https://doi.org/10.1007/s11094-005-0142-8
8. Pahontu, E., Fala, V., Gulea, A., Poirier, D., Tapcov, V., Rosu, T., *Molecules*, 2013, vol. 18, no. 8, p. 8812. https://doi.org/10.3390/molecules18088812
9. Bindu, P., Kurup, M.R.P., and Satyakeerty, T.R., *Polyhedron*, 1998, vol. 18, nos. 3–4, p. 321. https://doi.org/10.1016/S0277-5387(98)00166-1
10. Zhang, Z., Gou, Y., Wang, J., Yang, K., Qi, J., Zhou, Z., Liang, Sh., Liang, H., and Yang, F., *Eur. J. Med. Chem*., 2016, vol. 121, p. 399. https://doi.org/10.1016/j.ejmech.2016.05.021
11. Orysyk, S.I., Repich, G.G., Bon, V.V., Dyakonenko, V.V., Orysyk, V.V., Zborovskii, Yu.L., Shishkin, O.V., Pekhnyo, V.I., and Vovk, M.V., *Inorg. Chim. Acta*, 2014, vol. 423A, p. 496. https://doi.org/10.1016/j.ica.2014.08.056
12. Bon', V.V., Orysyk, S.I., and Pekhno, V.I., *Russ. J. Coord. Chem*., 2011, vol. 37, no. 2, p. 149. https://doi.org/10.1134/S1070328411010027
13. Allen, F.H., *Acta Crystallogr. (A)*, 2002, vol. 58, p. 380. https://doi.org/10.1107/S0108768102003890
14. CrysAlis RED, Oxford Diffraction Ltd., Version 1.171.34.76, 2003.
15. Sheldrich, G.M., *Acta Crystallogr. (A)*, 2008, vol. 64, p. 112. https://doi.org/10.1107/S0108767307043930
16. Gulea, A., Poirier, D., Roy, J., Stavila, V., Bulimestru, I., Tapcov, V., and Popovschi, L., *J. Enzyme Inhib. Med. Chem*., 2008, vol. 23, no. 6, p. 806. https://doi.org/10.1080/14756360701743002
17. Balan, G., Burduniuc, O., Usataia, I., Graur, V., Chumakov, Yu., Petrenko, P., Gudumac, V., Gulea, A., and Pahontu, E., *Appl. Organometal. Chem*., 2020, vol. 34, no. 3, p. e5423. https://doi.org/10.1002/aoc.5423
18. Orysyk, S.I., Bon, V.V., Zholob, O.O., Pekhnyo, V.I., Orysyk, V.V., Zborovskii, Y.L., and Vovk, M.V., *Polyhedron*, 2013, vol. 51, p. 211. https://doi.org/10.1016/j.poly.2012.12.021